The Colour Glass Condensate 4

Edmond Iancu
Institut de Physique Théorique de Saclay

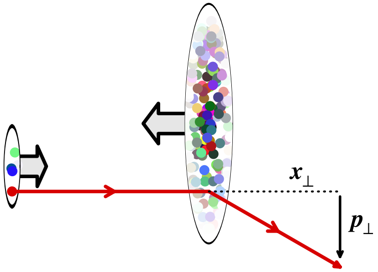

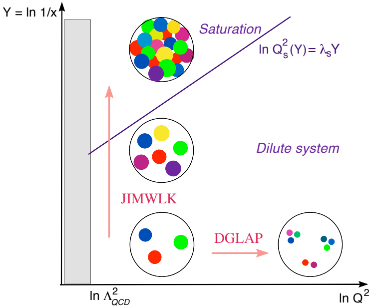

The BK equation *(Balitsky, '96; Kovchegov, '99)*

$$\frac{\partial S_Y(\boldsymbol{x},\boldsymbol{y})}{\partial Y} = \frac{\bar{\alpha}}{2\pi}\int \mathrm{d}^2\boldsymbol{z}\,\mathcal{M}_{\boldsymbol{xyz}}\big[S_Y(\boldsymbol{x},\boldsymbol{z})S_Y(\boldsymbol{z},\boldsymbol{y}) - S_Y(\boldsymbol{x},\boldsymbol{y})\big]$$

- Convenient notation: $\bar{\alpha} \equiv \alpha_s N_c/\pi$ (fixed coupling for now)
- Dipole kernel $\mathcal{M}_{\boldsymbol{xyz}}$: BFKL kernel in the dipole picture *(Al Mueller, 1990)*

$$\mathcal{M}_{\boldsymbol{xyz}} = \frac{(\boldsymbol{x}-\boldsymbol{y})^2}{(\boldsymbol{x}-\boldsymbol{z})^2(\boldsymbol{y}-\boldsymbol{z})^2} = \left[\frac{z^i - x^i}{(\boldsymbol{z}-\boldsymbol{x})^2} - \frac{z^i - y^i}{(\boldsymbol{z}-\boldsymbol{y})^2}\right]^2$$

- The sum of the emission probabilities for the 4 possible gluon attachements :

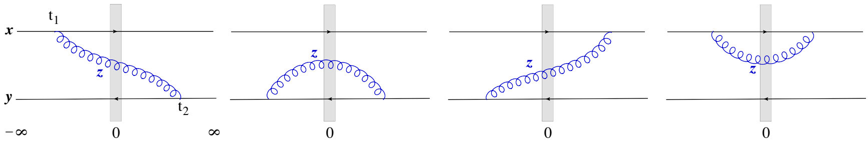

The Weisäcker-Williams classical field: $A^i_a(\boldsymbol{z}) = \frac{1}{2\pi}\,\frac{z^i - x^i}{(\boldsymbol{z}-\boldsymbol{x})^2}\,t^a$

The dipole kernel

$$\mathcal{M}_{\boldsymbol{xyz}} = \frac{(\boldsymbol{x}-\boldsymbol{y})^2}{(\boldsymbol{x}-\boldsymbol{z})^2(\boldsymbol{y}-\boldsymbol{z})^2} = \left[\frac{z^i - x^i}{(\boldsymbol{z}-\boldsymbol{x})^2} - \frac{z^i - y^i}{(\boldsymbol{z}-\boldsymbol{y})^2}\right]^2$$

- Colour transparency: $\mathcal{M}_{\boldsymbol{xyz}} \to 0$ when $r = |\boldsymbol{x}-\boldsymbol{y}| \to 0$
- Infrared safety: rapid decrease of the emission probability at large $z_\perp$

$$\mathcal{M}_{\boldsymbol{xyz}} \simeq \frac{r^2}{(\boldsymbol{z}-\boldsymbol{x})^4} \quad \text{when } |\boldsymbol{z}-\boldsymbol{x}| \simeq |\boldsymbol{z}-\boldsymbol{y}| \gg r$$

  - cancellations between self-energy (qq or $\bar{q}\bar{q}$) and exchange ($q\bar{q}$) graphs

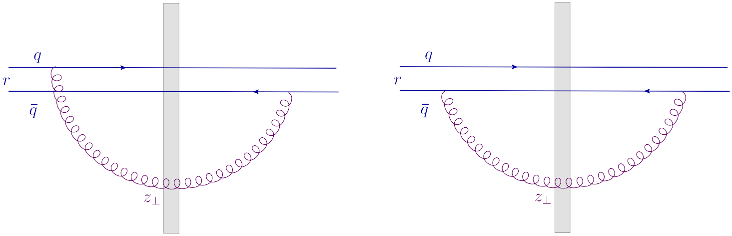

The dipole kernel

$$\mathcal{M}_{\boldsymbol{xyz}} = \frac{(\boldsymbol{x}-\boldsymbol{y})^2}{(\boldsymbol{x}-\boldsymbol{z})^2(\boldsymbol{y}-\boldsymbol{z})^2} = \left[\frac{z^i - x^i}{(\boldsymbol{z}-\boldsymbol{x})^2} - \frac{z^i - y^i}{(\boldsymbol{z}-\boldsymbol{y})^2}\right]^2$$

- Colour transparency: $\mathcal{M}_{\boldsymbol{xyz}} \to 0$ when $r = |\boldsymbol{x}-\boldsymbol{y}| \to 0$
- Infrared safety: rapid decrease of the emission probability at large $z_\perp$

$$\mathcal{M}_{\boldsymbol{xyz}} \simeq \frac{r^2}{(\boldsymbol{z}-\boldsymbol{x})^4} \quad \text{when } |\boldsymbol{z}-\boldsymbol{x}| \simeq |\boldsymbol{z}-\boldsymbol{y}| \gg r$$

  - cancellations between self-energy (qq or $\bar{q}\bar{q}$) and exchange ($q\bar{q}$) graphs
- Short-distance poles ($\boldsymbol{z} = \boldsymbol{x}$) cancel between 'crossing' and 'non-crossing'

$$\boldsymbol{z} \to \boldsymbol{x} \implies S_Y(\boldsymbol{x},\boldsymbol{z})S_Y(\boldsymbol{z},\boldsymbol{y}) \to \mathbb{I} \times S_Y(\boldsymbol{x},\boldsymbol{y})$$

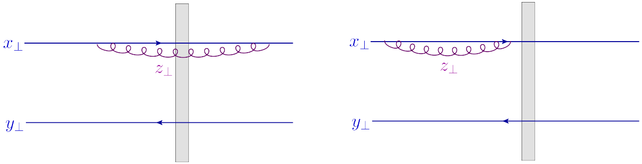

BFKL & Unitarity

- Non-linear generalization of the BFKL equation for $T_{\boldsymbol{xy}} \equiv 1 - S_{\boldsymbol{xy}}$

$$\frac{\partial T_{\boldsymbol{xy}}}{\partial Y} = \frac{\bar{\alpha}}{2\pi} \int \mathrm{d}^2\boldsymbol{z}\, \mathcal{M}_{\boldsymbol{xyz}} \big[T_{\boldsymbol{xz}} + T_{\boldsymbol{zy}} - T_{\boldsymbol{xy}} - T_{\boldsymbol{xz}} T_{\boldsymbol{zy}} \big]$$

- Non-linear term T^2: the simultaneous scattering of both daughter dipoles
- When scattering is weak, $T \ll 1$, one recovers the linear BFKL equation
  - exponential increase with Y leading to unitarity violation
- The non-linear term in BK restores unitarity: $T(r, Y) \leq 1$ for any r and Y
  - $T = 0$ (no scattering) and $T = 1$ (total absorption) are fixed points
- Saturation momentum $Q_s(Y)$: $T(r, Y) = 0.5$ when $r = 1/Q_s(Y)$
  - $Q_s(Y)$ increases rapidly with Y due to the BFKL dynamics

The saturation front

- Numerical solutions to BK with initial condition from the MV model
- Logarithmic variable $\rho \equiv \ln(1/r^2 Q_0^2) \Longrightarrow$ large $\rho \leftrightarrow$ small r

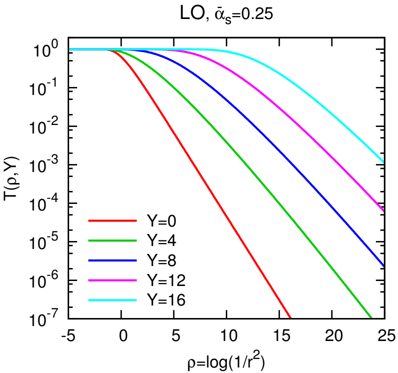

$$T(r, Y=0) = 1 - \mathrm{e}^{-\frac{r^2 Q_0^2}{4} \ln \frac{1}{r^2 \Lambda^2}}$$

$$T(\rho_s(Y), Y) = 0.5 \quad \text{for} \quad \rho_s(Y) = \lambda_s Y$$

$$T(\rho, Y) \simeq \begin{cases} \mathrm{e}^{-\gamma_s(\rho - \rho_s)} & (\rho > \rho_s) \\ 1 & (\rho \lesssim \rho_s) \end{cases}$$

- Geometric scaling: $T(r, Y) \simeq \left(r^2 Q_s^2(Y)\right)^{\gamma_s}$ with $\gamma_s \simeq 0.63$
  - a front which preserves its shape while progressing to larger values of ρ

- Numerical solutions to BK with initial condition from the MV model
- Logarithmic variable $\rho \equiv \ln(1/r^2 Q_0^2) \Longrightarrow$ large $\rho \leftrightarrow$ small r

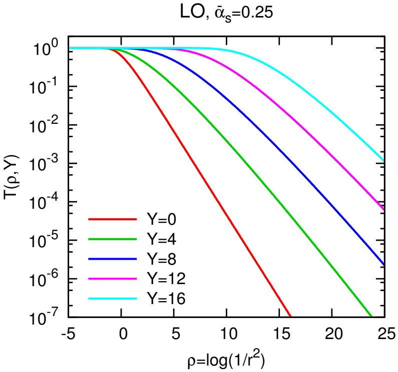

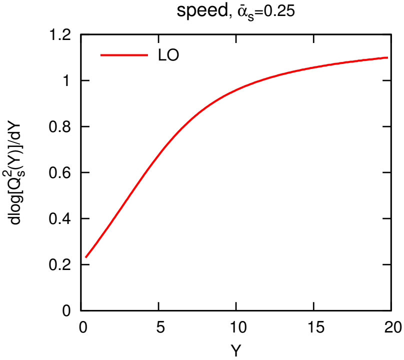

- Saturation exponent: the speed of the saturation front

$$\lambda_s \equiv \frac{\mathrm{d}\rho_s}{\mathrm{d}Y} \simeq 4.88\bar{\alpha} - \frac{1}{2\gamma_s Y}\,, \qquad Q_s^2(Y) \simeq Q_0^2\,\mathrm{e}^{\lambda_s Y}$$

The saturation front

- Numerical solutions to BK with initial condition from the MV model
- Logarithmic variable $\rho \equiv \ln(1/r^2 Q_0^2) \Longrightarrow$ large $\rho \leftrightarrow$ small r

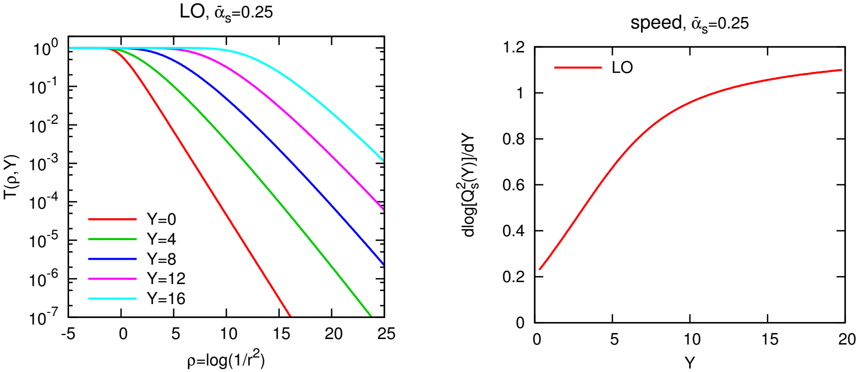

- These properties have been independently established in

  E.I., K. Itakura, L. McLerran, hep-ph/0203137;
  A.H. Mueller, D.N. Triantafyllopoulos, hep-ph/0205167

More on the saturation exponent

- Leading order BK qualitatively explain geometric scaling at HERA ...
- But the growth of the saturation momentum is too fast: $\lambda_s \simeq 4.88\bar{\alpha} \sim 1$

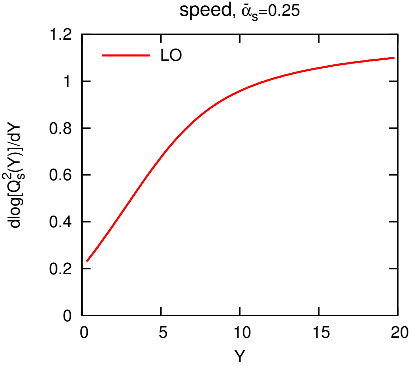

- Remember: HERA data

$$Q_s^2(x) \simeq \alpha_s \frac{xG(x, Q_s^2)}{\pi R^2} \sim \frac{1}{x^{\lambda_s}}$$

with $\lambda_s \simeq 0.2 \div 0.3$

More on the saturation exponent

- Leading order BK qualitatively explain geometric scaling at HERA ...
- But the growth of the saturation momentum is too fast: $\lambda_s \simeq 4.88\bar{\alpha} \sim 1$

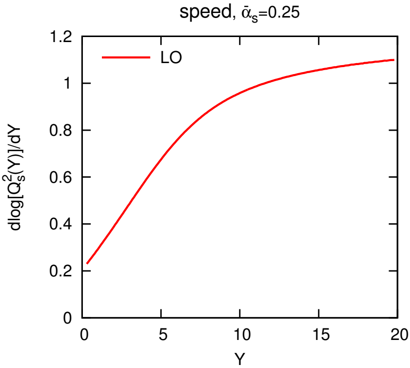

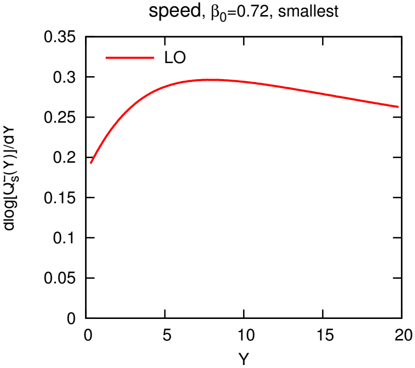

- Using a running coupling dramatically slows down the evolution
  - $\alpha_s(Q_s^2(Y))$ decreases with Y
- Rather successful phenomenology based on rcBK

- Leading order BK qualitatively explain geometric scaling at HERA ...
- But the growth of the saturation momentum is too fast: $\lambda_s \simeq 4.88\bar{\alpha} \sim 1$

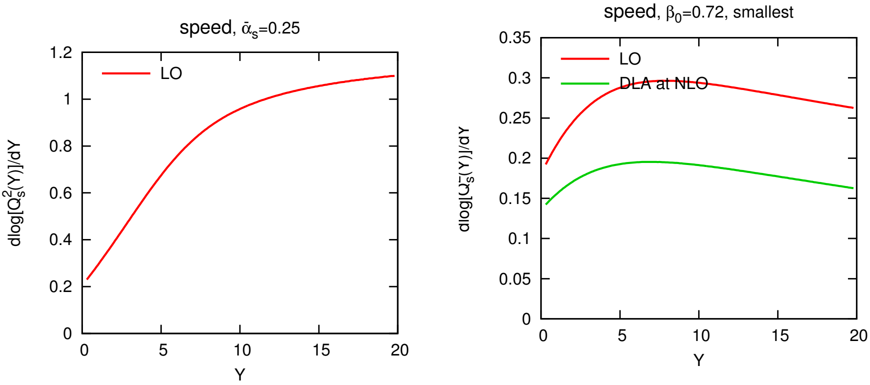

- Adding NLO corrections further reduces the saturation exponent: $\lambda_s \simeq 0.2$

  D.N. Triantafyllopoulos, hep-ph/0209121

Forward hadron production in pA from the CGC

- Recall: Forward production probes small x gluons in nucleus A

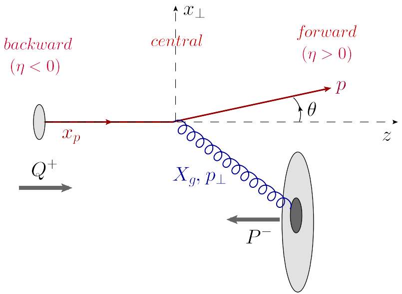

$$x_p = \frac{p_\perp}{\sqrt{s}}\, e^{\eta}$$

$$X_g = \frac{p_\perp}{\sqrt{s}}\, e^{-\eta}$$

$X_g \ll x_p$ when $\eta > 0$

- Rich phenomenology:
  - d+Au collisions at RHIC (BRAHMS, STAR...)
  - p+Pb collisions at the LHC (ALICE, ATLAS, LHCb...)
- Some intriguing data, naturally explained by gluon saturation and the CGC
- State-of-the art: CGC fits to next-to-leading order (NLO) accuracy

The nuclear modification factor at RHIC

$$R_{pA} \equiv \frac{1}{A^{1/3}} \frac{\mathrm{d}N_{pA}/\mathrm{d}^2p_\perp \mathrm{d}\eta}{\mathrm{d}N_{pp}/\mathrm{d}^2p_\perp \mathrm{d}\eta} = \frac{1}{A^{1/3}} \frac{\tilde{S}_A(p_\perp, X_g)}{\tilde{S}_p(p_\perp, X_g)}$$

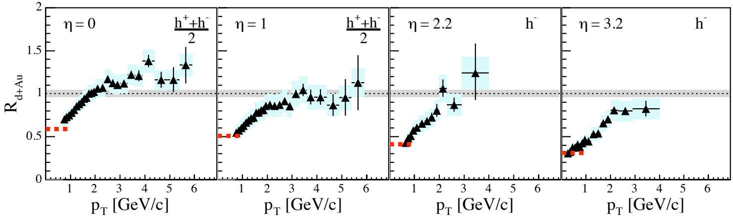

- Numerical solution to rcBK *(BK equation: Albacete et al, hep-ph/0307179)*

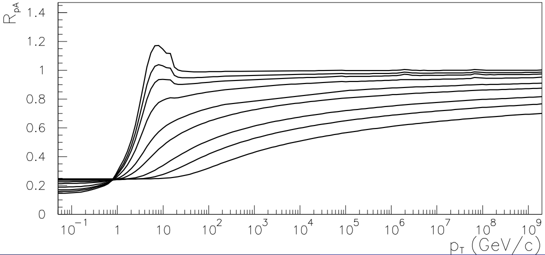

$$\tilde{S}(p_\perp, X_g) = \int_{\boldsymbol{r}} \mathrm{e}^{-\mathrm{i}\boldsymbol{r}\cdot\boldsymbol{p}}\, S(\boldsymbol{r}, X_g)$$

$$X_g = \frac{p_\perp}{\sqrt{s}}\, \mathrm{e}^{-\eta}$$

$\eta =$ 0, 0.05, 0.1, 0.2, ... up to 2

Early fits to RHIC data

- Hybride factorisation at leading-order + ad-hoc K-factor (fit)

$$\left.\frac{\mathrm{d}N_h}{\mathrm{d}\eta\,\mathrm{d}^2\boldsymbol{k}}\right|_{\mathrm{LO}} = K_h \int_{x_p}^{1} \frac{\mathrm{d}z}{z^2}\,\frac{x_p}{z} q\left(\frac{x_p}{z}\right) \tilde{\mathcal{S}}\left(\frac{\boldsymbol{k}}{z}, X_g\right) D_{h/q}(z)$$

  - quark distribution in the deuteron
  - dipole S–matrix from solutions to BK equation with running coupling
  - initial condition from the MV model (fit parameters)
  - quark fragmentation into hadrons in the final state

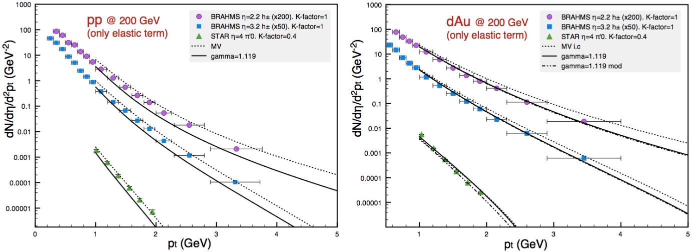

(Albacete, Dumitru, Fujii, Nara, arXiv:1209.2001)

Forward particle production in pA at NLO

- NLO calculation of the "impact factor" : additional gluon emission

  Chirilli, Xiao and Yuan, arXiv:1203.6139, Phys. Rev. D

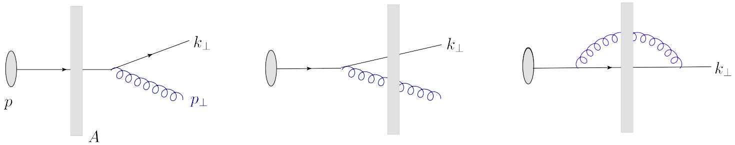

- A puzzle: negative cross-section *(Stasto, Xiao, Zaslavsky, 1307.4057)*

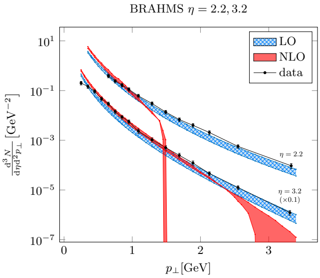

- Data from RHIC
- Good agrement at small $p_\perp$
- Suddenly negative at $p_\perp \gtrsim Q_s$
- Issue with subtracting the LO

Forward particle production in pA at NLO

- NLO calculation of the "impact factor" : additional gluon emission
  Chirilli, Xiao and Yuan, arXiv:1203.6139, Phys. Rev. D

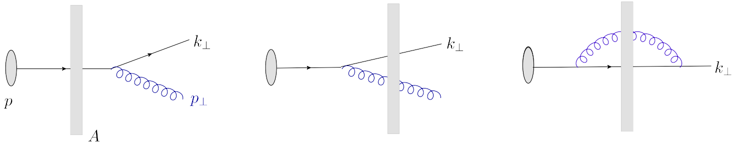

- ... and its solution *(E.I., A. Mueller, D. Triantafyllopoulos, 1608.05293)*

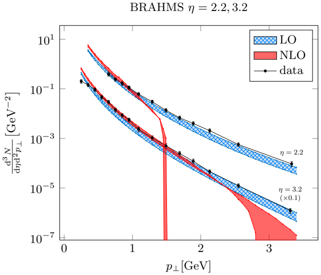

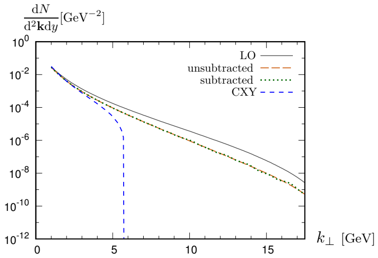

- Numerics by *Ducloué, Lappi, and Zhu, arXiv:1703.04962*

Recent fits at NLO

- *Shi, Wang, Wei, and Xiao, arXiv:2112.06975, PRL*

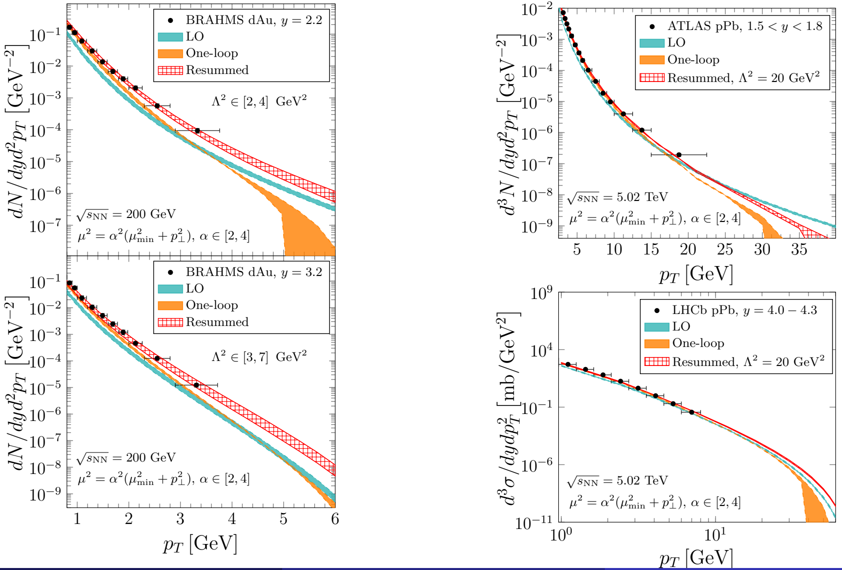

Forward di-hadron production in pA collisions

- Multiple scattering can also affect angular correlations in the final state
- Di-hadron production in pA collisions at forward rapidities: $\eta_1,\, \eta_2 > 1$
- The quark from the proton radiates a gluon prior to, or after, the scattering

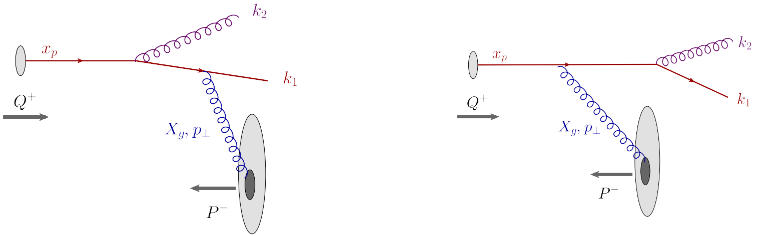

$$x_p = \frac{k_{1\perp}}{\sqrt{s}}\,\mathrm{e}^{\eta_1} + \frac{k_{2\perp}}{\sqrt{s}}\,\mathrm{e}^{\eta_2} \sim \mathcal{O}(1)\,, \qquad X_g = \frac{k_{1\perp}}{\sqrt{s}}\,\mathrm{e}^{-\eta_1} + \frac{k_{2\perp}}{\sqrt{s}}\,\mathrm{e}^{-\eta_2} \ll 1$$

- Collinear factorization : $\boldsymbol{k}_{1\perp} + \boldsymbol{k}_{2\perp} \simeq 0 \Longrightarrow$ a peak at $\Delta\phi = \phi_2 - \phi_1 = \pi$
  - a pair of hadrons propagating back-to-back in the transverse plane

Forward di-hadron production in pA collisions

- Multiple scattering can also affect angular correlations in the final state
- Di-hadron production in pA collisions at forward rapidities: $\eta_1,\, \eta_2 > 1$
- The quark from the proton radiates a gluon prior to, or after, the scattering

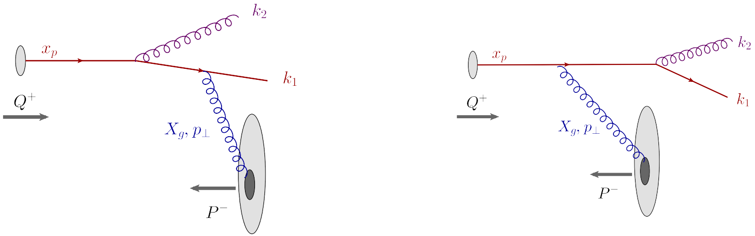

- In the presence of gluon saturation: $|\boldsymbol{k}_{1\perp} + \boldsymbol{k}_{2\perp}| \simeq Q_s(X_g)$
  - a broadening $\delta\phi \sim Q_s/k_\perp$ of the peak at $\Delta\phi = \pi$
- Measure pairs of particles and extract their correlation in azimuthal angle

$$\mathcal{C}(\Delta\phi) \equiv \frac{\mathrm{d}N_{\rm pair}}{\mathrm{d}^2k_{1\perp}\mathrm{d}\eta_1\mathrm{d}^2k_{2\perp}\mathrm{d}\eta_2} - \frac{\mathrm{d}N}{\mathrm{d}^2k_{1\perp}\mathrm{d}\eta_1}\,\frac{\mathrm{d}N}{\mathrm{d}^2k_{2\perp}\mathrm{d}\eta_2}$$

Di–hadrons at RHIC: p+p vs. d+Au

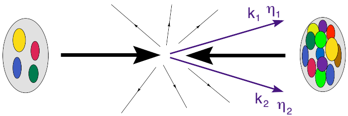

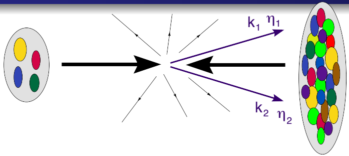

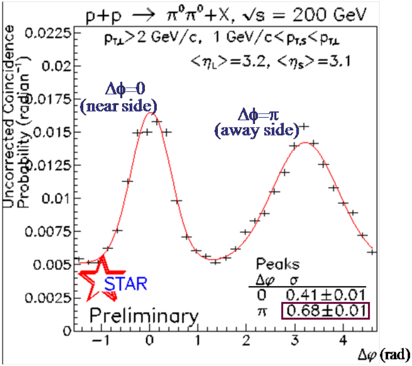

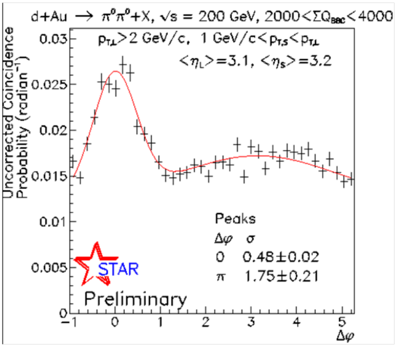

- Significant broadening even in pp collisions: recoil in jet fragmentation
- Forward rapidities: $\eta_1, \eta_2 \sim 3 \Longrightarrow x_p \sim 0.5$, but $X_g \sim 10^{-3}$

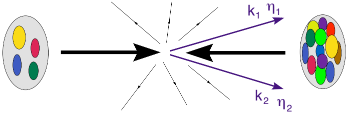

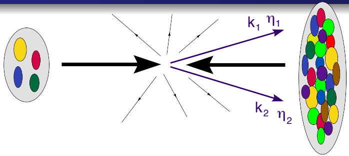

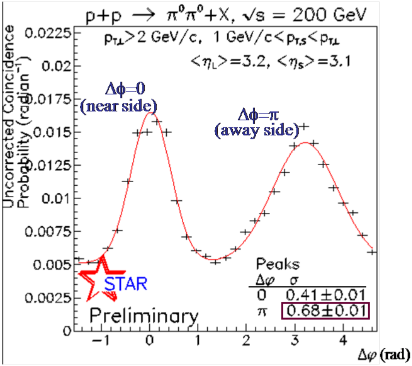

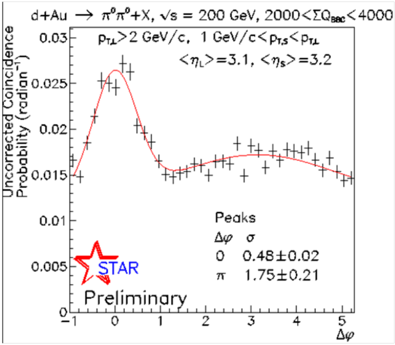

- The broadening in d+Au is considerably stronger than that in pp
- Predicted by the CGC *(Marquet, 2007; Albacete and Marquet, 2010)*

- The collinear quark radiates a gluon prior to, or after, the scattering

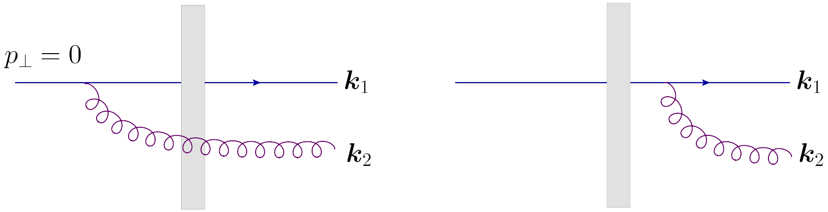

- Up to four Wilson lines in the cross–section
- At large N_c, this factorizes into color dipoles and quadrupoles

$$\langle Q_{\boldsymbol{x}_1\boldsymbol{x}_2\boldsymbol{x}_3\boldsymbol{x}_4}\rangle_Y = \frac{1}{N_c}\langle \mathrm{tr}(V^\dagger_{\boldsymbol{x}_1}V_{\boldsymbol{x}_2}V^\dagger_{\boldsymbol{x}_3}V_{\boldsymbol{x}_4})\rangle_Y$$

- This property holds for any multi-particle final state at large N_c

  (Kovner and Lublinsky, 2012; Dominguez, Marquet, Stasto, and Xiao, '12)

- How to compute the quadrupole ? Or even the dipole, but for $N_c = 3$?

The mean field approximation

- Gaussian Ansatz for $W_Y[\rho]$: "MV model with Y-dependent 2-point function"
  - all Wilson lines correlators (quadrupole etc) can be related to the dipole S-matrix, as obtained by solving the BK equation

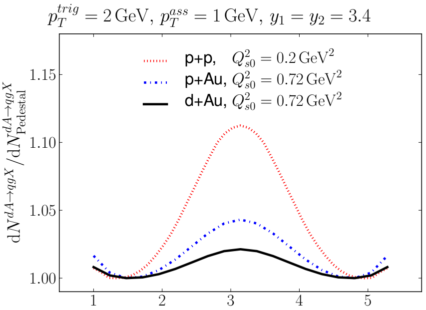

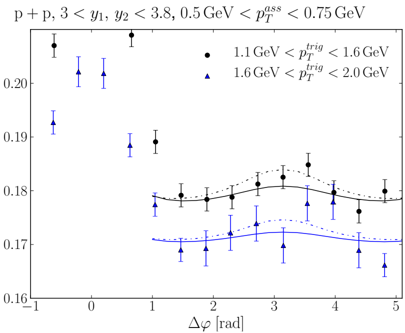

- Left: different combinations projectile–target

  (Lappi, Mäntysaari, 1209.2853; also Stasto, Wei, Xiao, Yuan, 1805.05712)

- Right: comparison with RHIC data for d+Au (PHENIX, 1105.5112)

JIMWLK evolution

(Jalilian-Marian, Iancu, McLerran, Weigert, Leonidov, and Kovner, 97–00)

- The relevant color charges at small-x (leading logarithmic approximation):
  - valence quarks + soft gluons with $1 \gg x' \gg x$
- $W_Y[\rho]$ is built by integrating out soft gluon fluctuations in (small) layers of x
  - $x' \to bx'$ with $b \ll 1$ but such that $\bar{\alpha}\ln(1/b) \ll 1$ as well
- Initial condition at low energy ($x_0 \sim 0.01$): MV model (valence quarks)

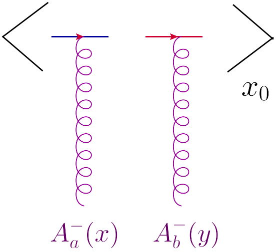

- independent color sources
- Gaussian weight function

$$W_0[\rho] = \mathcal{N} \exp\left\{-\int_{x^+,\boldsymbol{x}} \frac{\rho_a(x)\rho_a(x)}{\mu^2(x)}\right\}$$

- $\mu^2(x)$: density of color charge squared

JIMWLK evolution

(Jalilian-Marian, Iancu, McLerran, Weigert, Leonidov, and Kovner, 97–00)

- The relevant color charges at small-x (leading logarithmic approximation):
  - valence quarks + soft gluons with $1 \gg x' \gg x$
- $W_Y[\rho]$ is built by integrating out soft gluon fluctuations in (small) layers of x
  - $x' \to bx'$ with $b \ll 1$ but such that $\bar{\alpha}\ln(1/b) \ll 1$ as well
- One step in the quantum evolution $\Longrightarrow$ JIMWLK Hamiltonian

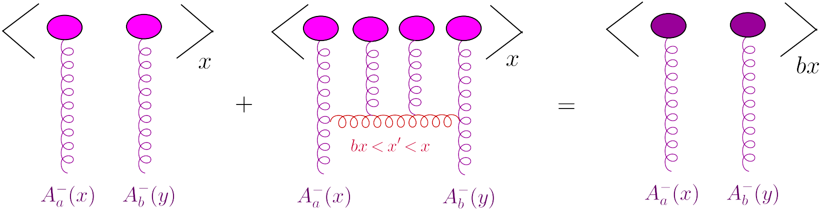

- The quantum gluon can scatter of the strong color fields generated in previous steps $\Longrightarrow$ non-linear evolution

JIMWLK evolution

(Jalilian-Marian, Iancu, McLerran, Weigert, Leonidov, and Kovner, 97–00)

- The relevant color charges at small-x (leading logarithmic approximation):
  - valence quarks + soft gluons with $1 \gg x' \gg x$
- $W_Y[\rho]$ is built by integrating out soft gluon fluctuations in (small) layers of x
  - $x' \to bx'$ with $b \ll 1$ but such that $\bar{\alpha}\ln(1/b) \ll 1$ as well
- One step in the quantum evolution $\Longrightarrow$ JIMWLK Hamiltonian

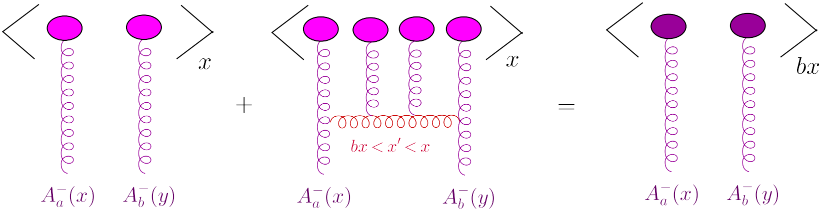

$$\frac{\partial W_Y[\rho]}{\partial Y} = H_{\rm JIMWLK}\left[\rho, \frac{\delta}{\delta\rho}\right] W_Y[\rho]$$ (a functional eq.)

JIMWLK evolution in Langevin form

- Useful to compare projectile (dipole) and target (nucleus) evolutions

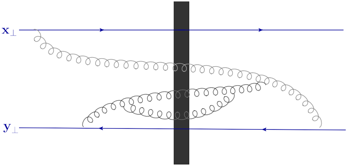

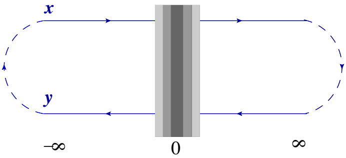

  - projectile: gluon emissions closer and closer to the target
  - target: color charges further and further away from the valence quarks

- Uncertainty principle: decreasing $x = k^-/P^- \leftrightarrow$ increasing $\Delta x^+ \sim 1/k^-$

- JIMWLK evolution builds the color charge distribution in layers of x^+

- New sources are one-loop quantum fluctuations
  - random variables with a Gaussian distribution
  - can equivalently be represented as a Gaussian noise

- A Langevin equation: random walk in the space of the Wilson lines

JIMWLK in Langevin form *(Blaizot, E.I., Weigert, '03)*

- Discretize the rapidity interval: $Y = n\epsilon$, $\epsilon \equiv \ln(1/b)$

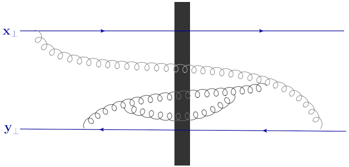

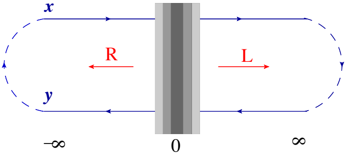

$$V_{\boldsymbol{x}}(n\varepsilon + \varepsilon) \;=\; \exp\big(i\varepsilon\alpha^a_{L\boldsymbol{x}}t^a\big)\, V_{\boldsymbol{x}}(n\varepsilon)\, \exp\big(-i\varepsilon\alpha^b_{R\boldsymbol{x}}t^b\big)$$

- $\alpha^a_{R,L}$: the change δA^-_a at larger negative (R) or positive (L) values of x^+

$$\alpha^a_{L\boldsymbol{x}} \;=\; g\int_{\boldsymbol{z}} \frac{x^i - z^i}{(\boldsymbol{x}-\boldsymbol{z})^2}\,\nu^{ia}_{\boldsymbol{z}}\,, \qquad \alpha^a_{R\boldsymbol{x}} \;=\; g\int_{\boldsymbol{z}} \frac{x^i - z^i}{(\boldsymbol{x}-\boldsymbol{z})^2}\,\tilde{V}^{ab}_{\boldsymbol{z}}\,\nu^{ib}_{\boldsymbol{z}}$$

- Noise ν^a: random color charge of the newly emitted gluon

$$\langle \nu^{ia}_{\boldsymbol{x}}(m\varepsilon)\nu^{jb}_{\boldsymbol{y}}(n\varepsilon)\rangle = \frac{1}{\varepsilon}\,\delta_{mn}\delta^{ij}\delta^{ab}\delta_{\boldsymbol{x}\boldsymbol{y}}$$

- Well suited for numerics: 2D lattice *(Weigert and Rummukainen, '03)*

- Several numerical implementations: *Weigert and Rummukainen, '03 Lappi (2011); Schenke et al (since 2012); Roiesnel (2016)*

- Here: the lattice calculation of the dipole S-matrix par T. Lappi (2011)

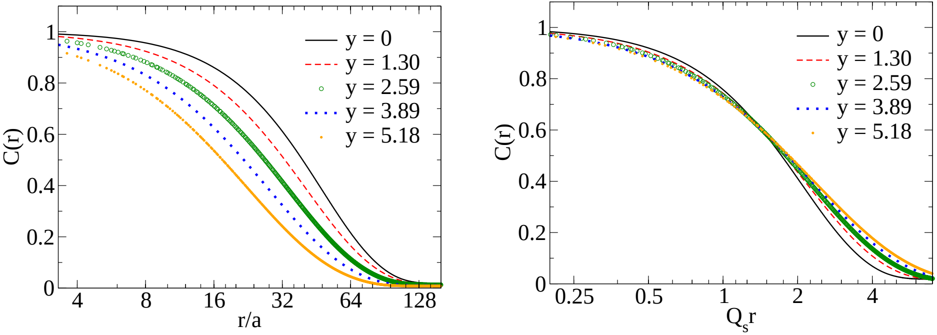

- $C(r) \equiv S(r, Y)$ as a function of r and of $rQ_s(Y)$ $\Longrightarrow$ geometric scaling

- Several numerical implementations: *Weigert and Rummukainen, '03 Lappi (2011); Schenke et al (since 2012); Roiesnel (2016)*

- Here: the lattice calculation of the dipole S-matrix par T. Lappi (2011)

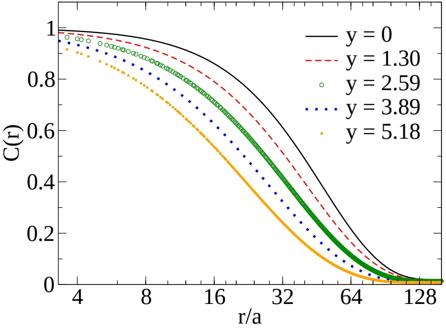

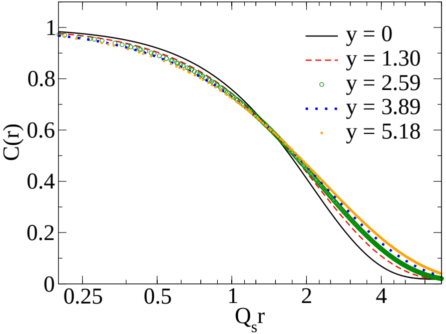

- A surprise: the large N_c approximation (BK for $S(r)$) turns out to be extremely good: error of order 1%, rather then the expected $10\% = 1/N_c^2$

Deconstructing DIS

- Recall: inclusive DIS at small x in the dipole picture
  - optical theorem: $\sigma_{\rm tot}$ is linear in the dipole scattering amplitude $T_{q\bar q}$

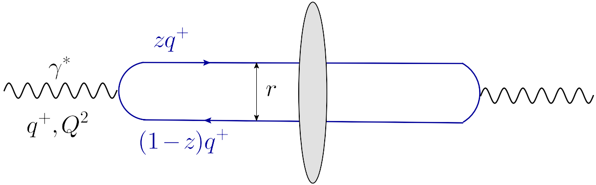

$$\sigma_{\rm tot}(Q^2,x) = \int {\rm d}^2 r \int_0^1 {\rm d}z \left|\Psi_{\gamma^*\to q\bar q}(r,z;Q^2)\right|^2 \underbrace{\sigma_{\rm dipole}(r,A,x)}_{2\pi R_A^2\, T(r,A,x)}$$

- What if we would like to measure the particles produced in the final state ?
  - at leading order : a quark-antiquark pair
  - after hadronisation: (at least) 2 hadrons or 2 jets
- One can measure both of them (dijets, dihadrons) or only one (semi-inclusive DIS): more detailed information about the target

Inclusive dijets in the back-to-back limit

(Dominquez, Marquet, Xiao, Yuan, 1101.0715)

- Inclusive dijets: a pair of jets plus everything else

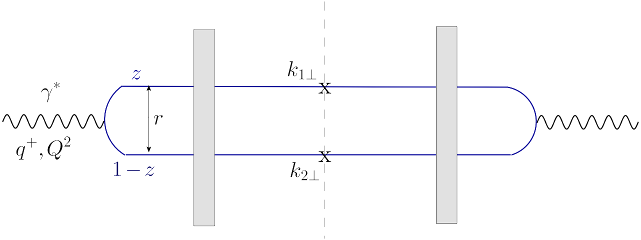

- Take the two jets to be relatively hard and nearly back-to-back

$$k_{1\perp} \simeq k_{2\perp} \;\gg\; K_\perp \equiv |\boldsymbol{k}_{1\perp} + \boldsymbol{k}_{2\perp}| \sim Q_s$$

- Why would this be interesting to study gluon saturation ?

- Azimuthal correlations: momentum imbalance $K_\perp$ fixed by the scattering
  - multiple scattering $\Rightarrow$ broadening of the peak at $\Delta\Phi = \pi$

Emergent TMD factorisation

- Two widely-separated transverse momentum scales: $P_\perp \gg K_\perp \gtrsim Q_s$

$$\boldsymbol{P}_\perp \equiv \frac{1}{2}(\boldsymbol{k}_{1\perp} - \boldsymbol{k}_{2\perp}) \ \text{(relative } p_T\text{)}, \quad \boldsymbol{K}_\perp \equiv \boldsymbol{k}_{1\perp} + \boldsymbol{k}_{2\perp} \ \text{(imbalance)}$$

- Photon virtuality Q^2 not so important: $P_\perp$ defines the hard scale
- Small $q\bar{q}$ dipole: $r = |\boldsymbol{x} - \boldsymbol{y}| \sim 1/P_\perp \ll 1/Q_s \implies$ single scattering

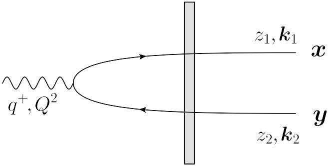

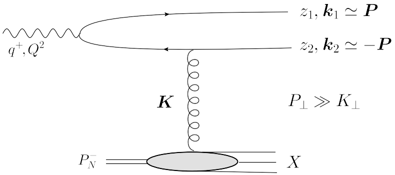

Emergent TMD factorisation

- Two widely-separated transverse momentum scales: $P_\perp \gg K_\perp \gtrsim Q_s$

$$\boldsymbol{P}_\perp \equiv \frac{1}{2}(\boldsymbol{k}_{1\perp} - \boldsymbol{k}_{2\perp}) \text{ (relative } p_T\text{)}, \quad \boldsymbol{K}_\perp \equiv \boldsymbol{k}_{1\perp} + \boldsymbol{k}_{2\perp} \text{ (imbalance)}$$

- Photon virtuality Q^2 not so important: $P_\perp$ defines the hard scale
- Small $q\bar{q}$ dipole: $r = |\boldsymbol{x} - \boldsymbol{y}| \sim 1/P_\perp \ll 1/Q_s \implies$ single scattering

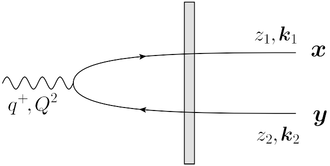

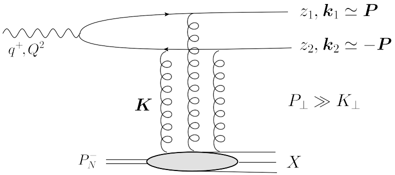

- Multiple scattering still important for the momentum imbalance: $K_\perp \sim Q_s$

$$V_{\boldsymbol{x}} V_{\boldsymbol{y}}^\dagger - 1 \simeq r^j \left(V_{\boldsymbol{b}} \partial^j V_{\boldsymbol{b}}^\dagger\right), \quad \boldsymbol{b} = (\boldsymbol{x} + \boldsymbol{y})/2$$

- $r \sim 1/P_\perp$ dependence factorises from the $b \sim 1/K_\perp$ dependence

Emergent TMD factorisation

- Two widely-separated transverse momentum scales: $P_\perp \gg K_\perp \gtrsim Q_s$

$$\boldsymbol{P}_\perp \equiv \frac{1}{2}(\boldsymbol{k}_{1\perp} - \boldsymbol{k}_{2\perp}) \;\; \text{(relative } p_T\text{)}, \quad \boldsymbol{K}_\perp \equiv \boldsymbol{k}_{1\perp} + \boldsymbol{k}_{2\perp} \;\; \text{(imbalance)}$$

- Photon virtuality Q^2 not so important: $P_\perp$ defines the hard scale
- Small $q\bar{q}$ dipole: $r = |\boldsymbol{x} - \boldsymbol{y}| \sim 1/P_\perp \ll 1/Q_s \implies$ single scattering

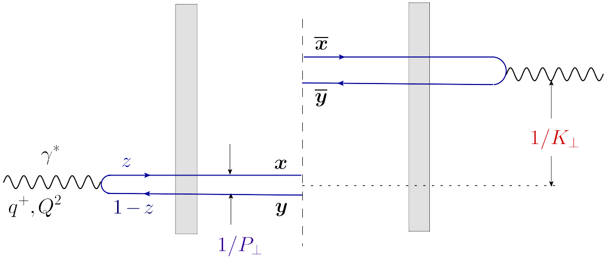

- Factorisation more suggestive in the transverse coordinate representation:
  - two small dipoles widely separated in impact parameter

TMD factorisation for inclusive dijets

$$\frac{\mathrm{d}\sigma^{\gamma^*_{T,L}A\to q\bar{q}A}}{\mathrm{d}z_1\mathrm{d}z_2\mathrm{d}^2\boldsymbol{P}\mathrm{d}^2\boldsymbol{K}} = H_{T,L}(z_1, z_2, Q^2, P_\perp^2)\,\mathcal{F}_{WW}(x, K_\perp^2)$$

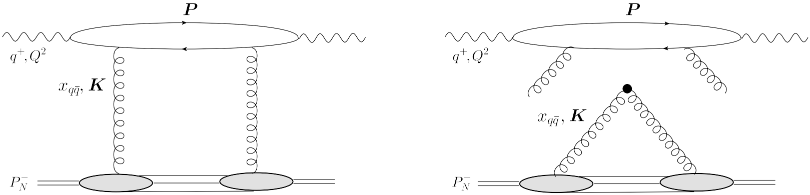

- Hard factor encoding the kinematics of the $q\bar{q}$ pair

$$H_T = \alpha_{em}\alpha_s e_f^2 \delta(1 - z_1 - z_2)\big(z_1^2 + z_2^2\big)\frac{P_\perp^4 + \bar{Q}^4}{(P_\perp^2 + \bar{Q}^2)^4} \qquad (\bar{Q}^2 = z_1 z_2 Q^2)$$

- Weiszäcker-Williams gluon TMD: unintegrated gluon distribution

$$\mathcal{F}_{WW}(x, K_\perp^2) = \int_{\boldsymbol{b},\bar{\boldsymbol{b}}} \frac{\mathrm{e}^{-i\boldsymbol{K}\cdot(\boldsymbol{b}-\bar{\boldsymbol{b}})}}{(2\pi)^4}\,\frac{-2}{\alpha_s}\Big\langle \mathrm{Tr}\Big[(\partial^i V_{\boldsymbol{b}})V_{\boldsymbol{b}}^\dagger(\partial^i V_{\bar{\boldsymbol{b}}})V_{\bar{\boldsymbol{b}}}^\dagger\Big]\Big\rangle_x$$

The Weiszäcker-Williams gluon TMD

- Gluon distribution $xG(x, Q^2)$: # of gluons with a given longitudinal momentum fraction x and transverse momenta $k_\perp \leq Q$ ... in the LC gauge

$$xG(x, Q^2) = \int \mathrm{d}^2\boldsymbol{k}_\perp \Theta(Q^2 - k_\perp^2) \int \mathrm{d}^2\boldsymbol{b}_\perp \; k^- \frac{\mathrm{d}^2 N_{gluon}}{\mathrm{d}k^- \mathrm{d}^2\boldsymbol{k}_\perp \mathrm{d}^2\boldsymbol{b}_\perp}\Big|_{k^-=xP^-}$$

- Occupation number $(\boldsymbol{r}_\perp = \boldsymbol{x}_\perp - \boldsymbol{y}_\perp,\ \boldsymbol{b} = (\boldsymbol{x}_\perp + \boldsymbol{y}_\perp)/2)$:

$$n(x, \boldsymbol{k}_\perp, \boldsymbol{b}_\perp) \;=\; \frac{1}{N_c^2-1} \int_{x^+, y^+} \int_{\boldsymbol{r}_\perp} \mathrm{e}^{-i\boldsymbol{k}_\perp \cdot \boldsymbol{r}_\perp} \langle F_a^{i-}(x^+, \boldsymbol{x}_\perp) F_a^{i-}(y^+, \boldsymbol{y}_\perp)\rangle\Big|_{A^-=0}$$

- However, color fields rotate under gauge transformations:

$$F_a^{i-}(x) \to U_{ab}(x) F_b^{i-}(x), \quad \text{with} \quad U(x) \in \mathrm{SU}(N_c)$$

The Weiszäcker-Williams gluon TMD

- Gluon distribution $xG(x, Q^2)$: # of gluons with a given longitudinal momentum fraction x and transverse momenta $k_\perp \le Q$ ... in the LC gauge

$$xG(x,Q^2) = \int \mathrm{d}^2\boldsymbol{k}_\perp \Theta(Q^2 - k_\perp^2) \int \mathrm{d}^2\boldsymbol{b}_\perp \; k^- \frac{\mathrm{d}^2 N_{gluon}}{\mathrm{d}k^- \mathrm{d}^2\boldsymbol{k}_\perp \mathrm{d}^2\boldsymbol{b}_\perp}\Big|_{k^-=xP^-}$$

- Generic gauge: insert a Wilson loop, to ensure gauge invariance:

$$n(x,\boldsymbol{k},\boldsymbol{b}) \;=\; \frac{1}{N_c^2-1}\int_{x^+,y^+}\int_{\boldsymbol{r}} \mathrm{e}^{-i\boldsymbol{k}\cdot\boldsymbol{r}} \big\langle F_a^{i-}(x^+,\boldsymbol{x})\,\mathcal{U}_\gamma^{ab}(x,y)\,F_b^{i-}(y^+,\boldsymbol{y})\big\rangle$$

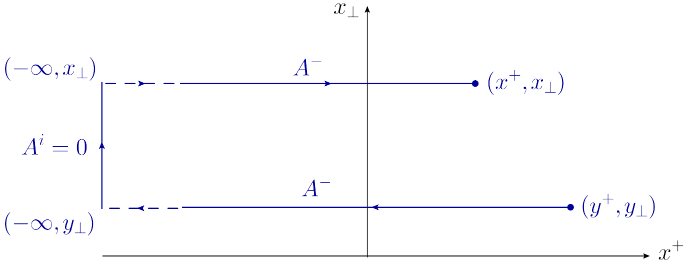

The Weiszäcker-Williams gluon TMD

- Gluon distribution $xG(x, Q^2)$: # of gluons with a given longitudinal momentum fraction x and transverse momenta $k_\perp \leq Q$ ... in the LC gauge

$$xG(x,Q^2) = \int \mathrm{d}^2\boldsymbol{k}_\perp \Theta(Q^2 - k_\perp^2) \int \mathrm{d}^2\boldsymbol{b}_\perp \; k^- \frac{\mathrm{d}^2 N_{gluon}}{\mathrm{d}k^- \mathrm{d}^2\boldsymbol{k}_\perp \mathrm{d}^2\boldsymbol{b}_\perp}\bigg|_{k^-=xP^-}$$

- $\tilde{A}^- = 0$ gauge: $\tilde{F}^{i-} = -\frac{\partial \tilde{A}^i}{\partial x^+}$ $\Rightarrow$ trivially integrate over x^+ and y^+

$$n(x,\boldsymbol{k},\boldsymbol{b}) \; = \; \frac{1}{N_c^2 - 1} \int_{\boldsymbol{r}} \mathrm{e}^{-i\boldsymbol{k}\cdot\boldsymbol{r}} \; \frac{-2}{g^2} \left\langle \mathrm{tr}\Big(V^\dagger \partial^i V(\boldsymbol{x})\Big)\Big(V^\dagger \partial^i V(\boldsymbol{y})\Big)\right\rangle_x$$

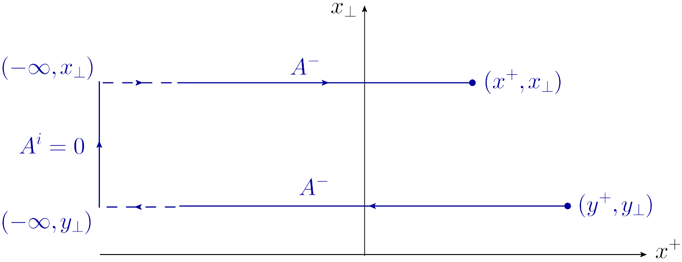

The Sudakov effect

- $P_\perp \gg K_\perp \Rightarrow$ large phase-space for final state emissions

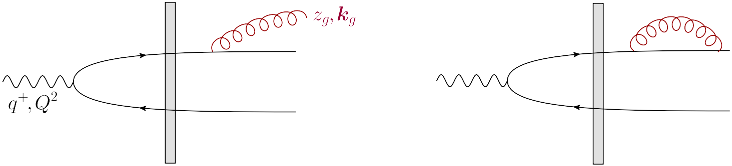

- Double-logarithmic integration: $K_\perp \ll k_{g\perp} \ll P_\perp$ and $z_g \ll 1$

- Virtual corrections dominate: suppression of the cross-section

$$\Delta\mathcal{F}_{\rm Sud}(x, K_\perp^2, P_\perp^2) = -\frac{\alpha_s N_c}{4\pi}\,\ln^2\frac{P_\perp^2}{K_\perp^2}\,\mathcal{F}_g(x, K_\perp^2)\,.$$

  - Physics: in order to keep a small imbalance $K_\perp \ll P_\perp$, one needs to suppress radiation *(Mueller, Xiao and Yuan, arXiv:1308.2993)*

- The one-loop result exponentiates: $\mathrm{e}^{-\Delta\mathcal{F}_{\rm Sud}}$

Azimuthal correlations in inclusive dijets

- $P_\perp \gg K_\perp$: azimuthal distribution shows a peak at $\Delta\phi = \pi$
- Dotted curves: additional broadening due to final-state radiation (Sudakov)

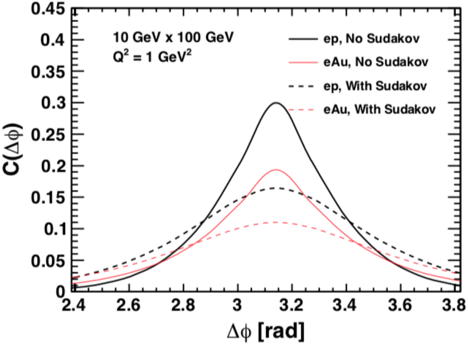

(Zheng, Aschenauer, Lee, and Xiao, arXiv:1403.2413)

- The effects of saturation are largely washed out ☹

Next-to-leading order

- Any effect of $\mathcal{O}\big(\bar{\alpha}^2 Y\big) \Longrightarrow \mathcal{O}(\bar{\alpha})$ correction to the r.h.s. of BK eq.

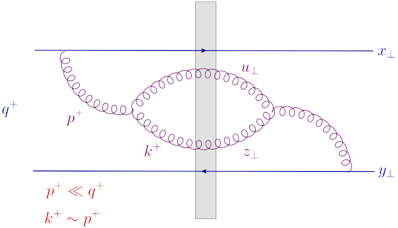

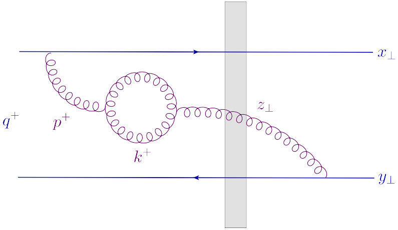

- The prototype: two successive, soft, emissions, with similar longitudinal momentum fractions: $p^+ \sim k^+ \ll q^+$
- Exact kinematics (full QCD vertices, as opposed to eikonal)
- Typically: two transverse momentum/coordinate convolutions: $\boldsymbol{u}_\perp$, $\boldsymbol{z}_\perp$
- New color structures, up to 3 dipoles at large N_c
- NLO BFKL: *Fadin, Lipatov, Camici, Ciafaloni ... 95-98*

BK equation at NLO *Balitsky, Chirilli (arXiv:0710.4330)*

$$\frac{\partial S_{\boldsymbol{xy}}}{\partial Y} = \frac{\bar{\alpha}}{2\pi}\int \mathrm{d}^2\boldsymbol{z}\,\frac{(\boldsymbol{x}-\boldsymbol{y})^2}{(\boldsymbol{x}-\boldsymbol{z})^2(\boldsymbol{y}-\boldsymbol{z})^2}\,\left(S_{\boldsymbol{xz}}S_{\boldsymbol{zy}} - S_{\boldsymbol{xy}}\right)\Bigg\{1 +$$

$$+\,\bar{\alpha}\left[\bar{b}\,\ln(\boldsymbol{x}-\boldsymbol{y})^2\mu^2 - \bar{b}\,\frac{(\boldsymbol{x}-\boldsymbol{z})^2-(\boldsymbol{y}-\boldsymbol{z})^2}{(\boldsymbol{x}-\boldsymbol{y})^2}\ln\frac{(\boldsymbol{x}-\boldsymbol{z})^2}{(\boldsymbol{y}-\boldsymbol{z})^2}\right.$$

$$\left.+\,\frac{67}{36}-\frac{\pi^2}{12}-\frac{1}{2}\ln\frac{(\boldsymbol{x}-\boldsymbol{z})^2}{(\boldsymbol{x}-\boldsymbol{y})^2}\ln\frac{(\boldsymbol{y}-\boldsymbol{z})^2}{(\boldsymbol{x}-\boldsymbol{y})^2}\right]\Bigg\}$$

$$+\,\frac{\bar{\alpha}^2}{8\pi^2}\int\frac{\mathrm{d}^2\boldsymbol{u}\,\mathrm{d}^2\boldsymbol{z}}{(\boldsymbol{u}-\boldsymbol{z})^4}\left(S_{\boldsymbol{xu}}S_{\boldsymbol{uz}}S_{\boldsymbol{zy}} - S_{\boldsymbol{xu}}S_{\boldsymbol{uy}}\right)$$

$$\Bigg\{-2+\frac{(\boldsymbol{x}-\boldsymbol{u})^2(\boldsymbol{y}-\boldsymbol{z})^2+(\boldsymbol{x}-\boldsymbol{z})^2(\boldsymbol{y}-\boldsymbol{u})^2-4(\boldsymbol{x}-\boldsymbol{y})^2(\boldsymbol{u}-\boldsymbol{z})^2}{(\boldsymbol{x}-\boldsymbol{u})^2(\boldsymbol{y}-\boldsymbol{z})^2-(\boldsymbol{x}-\boldsymbol{z})^2(\boldsymbol{y}-\boldsymbol{u})^2}\ln\frac{(\boldsymbol{x}-\boldsymbol{u})^2(\boldsymbol{y}-\boldsymbol{z})^2}{(\boldsymbol{x}-\boldsymbol{z})^2(\boldsymbol{y}-\boldsymbol{u})^2}$$

$$+\,\frac{(\boldsymbol{x}-\boldsymbol{y})^2(\boldsymbol{u}-\boldsymbol{z})^2}{(\boldsymbol{x}-\boldsymbol{u})^2(\boldsymbol{y}-\boldsymbol{z})^2}\left[1+\frac{(\boldsymbol{x}-\boldsymbol{y})^2(\boldsymbol{u}-\boldsymbol{z})^2}{(\boldsymbol{x}-\boldsymbol{u})^2(\boldsymbol{y}-\boldsymbol{z})^2-(\boldsymbol{x}-\boldsymbol{z})^2(\boldsymbol{y}-\boldsymbol{u})^2}\right]\ln\frac{(\boldsymbol{x}-\boldsymbol{u})^2(\boldsymbol{y}-\boldsymbol{z})^2}{(\boldsymbol{x}-\boldsymbol{z})^2(\boldsymbol{y}-\boldsymbol{u})^2}\Bigg\}$$

- green : leading-order (LO) terms
- violet : running coupling corrections ($\bar{b} = (11N_c - 2N_{\rm f})/12N_c$)
- blue : single collinear logarithm (DGLAP)
- red : double collinear logarithm : troublesome !

NLO : unstable numerical solutions

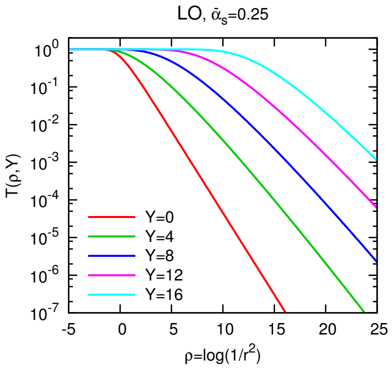

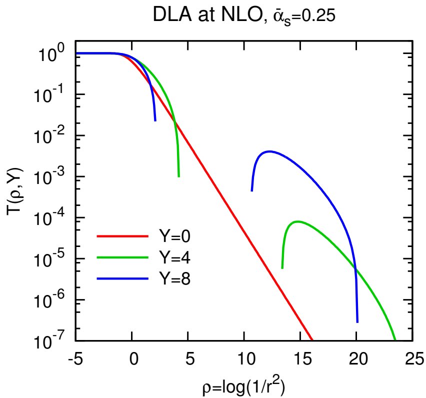

- Left: leading-order BK
- Right: LO BK + the double collinear logarithm alone
- Similar conclusion from full NLO BK *(Lappi, Mäntysaari, arXiv:1502.02400)*
- The source of instability: the double collinear logarithm

The double collinear logarithms

- Important when daughter dipoles are relatively large : gluons with low $k_\perp$

$$-\frac{1}{2}\ln\frac{(\boldsymbol{x}-\boldsymbol{z})^2}{(\boldsymbol{x}-\boldsymbol{y})^2}\ln\frac{(\boldsymbol{y}-\boldsymbol{z})^2}{(\boldsymbol{x}-\boldsymbol{y})^2}\simeq-\frac{1}{2}\ln^2\frac{(\boldsymbol{x}-\boldsymbol{z})^2}{r^2}\quad\text{if}\quad|\boldsymbol{z}-\boldsymbol{x}|\simeq|\boldsymbol{z}-\boldsymbol{y}|\gg r$$

- Generated by integrating out one gluon (at $\boldsymbol{u}$) whose size is intermediate:

$$|\boldsymbol{z}-\boldsymbol{x}|\simeq|\boldsymbol{z}-\boldsymbol{y}|\simeq|\boldsymbol{z}-\boldsymbol{u}|\gg|\boldsymbol{u}-\boldsymbol{x}|\simeq|\boldsymbol{u}-\boldsymbol{y}|\gg r$$

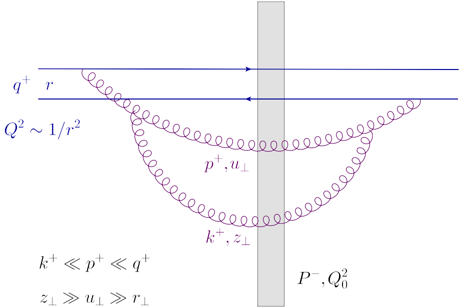

The double collinear logarithms

- Important when daughter dipoles are relatively large : gluons with low $k_\perp$

$$-\frac{1}{2}\ln\frac{(\boldsymbol{x}-\boldsymbol{z})^2}{(\boldsymbol{x}-\boldsymbol{y})^2}\ln\frac{(\boldsymbol{y}-\boldsymbol{z})^2}{(\boldsymbol{x}-\boldsymbol{y})^2}\simeq -\frac{1}{2}\ln^2\frac{(\boldsymbol{x}-\boldsymbol{z})^2}{r^2}\quad \text{if}\quad |\boldsymbol{z}-\boldsymbol{x}|\simeq|\boldsymbol{z}-\boldsymbol{y}|\gg r$$

- Keeping just the double collinear logarithms (notation: $|\boldsymbol{z}-\boldsymbol{x}|\to z$):

$$\frac{\partial T(Y,r)}{\partial Y}=\bar{\alpha}\int_{r^2}^{1/Q_0^2}\mathrm{d}z^2\,\frac{r^2}{z^4}\left\{1-\frac{\bar{\alpha}}{2}\ln^2\frac{z^2}{r^2}\right\}T(Y,z)$$

- The upper limit: $z=1/Q_0$ with Q_0 the target saturation scale at low energy
- The r.h.s. becomes negative if $r^2Q_0^2$ is small enough
- The typical situation for dilute-dense scattering at high-energy

$$\frac{1}{r^2}\sim Q_s^2(Y)=Q_0^2\,\mathrm{e}^{\lambda_s Y}\gg Q_0^2$$

Time ordering

- Successive emissions are ordered in k^+, by construction
- They should be also ordered in lifetimes ... but this condition is not enforced in perturbation theory and may be violated

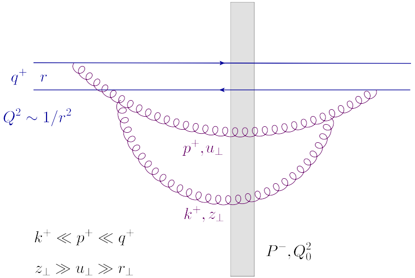

- lifetime of a gluon fluctuation:

$$\Delta t_p \simeq \frac{2p^+}{p_\perp^2} \sim p^+ u_\perp^2$$

- time-ordering condition:

$$\Delta t_p \sim p^+ u_\perp^2 \;>\; \Delta t_k \sim k^+ z_\perp^2$$

- violated when $z_\perp$ is large enough

- The correct time-ordering is eventually restored via quantum corrections, but only order-by-order
- The loop corrections restoring TO are enhanced by double collinear logs

Time ordering

- Integrate out the harder gluon $(p^+, u_\perp)$ to double-log accuracy:
- Without time-ordering (usual perturbation theory)

$$\bar{\alpha}\int_{k^+}^{q^+}\frac{\mathrm{d}p^+}{p^+}\int_{r^2}^{z^2}\frac{\mathrm{d}u^2}{u^2} = \bar{\alpha}\Delta Y \ln\frac{z^2}{r^2}\,, \qquad \Delta Y \equiv \ln\frac{q^+}{k^+}$$

  - $\mathcal{O}(\bar{\alpha}\Delta Y)$: one step in the leading-order evolution

- After also enforcing time-ordering:

$$\bar{\alpha}\int_{k^+}^{q^+}\frac{\mathrm{d}p^+}{p^+}\int_{r^2}^{z^2}\frac{\mathrm{d}u^2}{u^2}\,\Theta(p^+u^2 - k^+z^2) = \bar{\alpha}\Delta Y \ln\frac{z^2}{r^2} - \frac{\bar{\alpha}}{2}\ln^2\frac{z^2}{r^2}$$

  - the first term, linear in ΔY, counts for the LO evolution
  - the 2nd term does not (no ΔY): "pure NLO" ... but transverse log
  - it contributes to the NLO evolution after the integration over $(k^+, \boldsymbol{z})$

Resumming the double collinear logs

- Different pieces generated by TO are formally treated as different orders
  - an infinite series of terms enhanced by powers of double collinear logs
- This whole series can be resummed by enforcing TO within LO BK eq.
  - modified ("collinearly improved") version of the BK equation

(G. Beuf, 2014; E.I., Madrigal, Mueller, Soyez, and Triantafyllopoulos, 2015)

- Alternatively: reformulate the evolution in terms of the "target rapidity" η

$$Y = \ln\frac{q^+}{k^+} \longrightarrow \eta \equiv \ln\frac{P^-}{k^-} = \ln\frac{\tau_k}{\tau_0}\,, \quad \tau_k = \frac{1}{k^-} = \frac{2k^+}{k_\perp^2}\,, \quad \tau_0 = \frac{1}{P^-}$$

  - ordering in $\eta \Longleftrightarrow$ ordering in lifetimes
  - the proper time-ordering is automatically satisfied ☺
  - longitudinal phase-space: $\Delta\eta = \ln\frac{P^-}{q^-} = \ln\frac{1}{x_{\rm Bj}}$

(Ducloué, E.I., Mueller, Soyez, and Triantafyllopoulos, arXiv:1902.06637)

- $\lambda_s \equiv \frac{\mathrm{d}\ln Q_s^2}{\mathrm{d}\eta}$: the speed of the saturation front in η
  - recall: LO result $\lambda_s \simeq 4.88\bar{\alpha}$ (way too large)

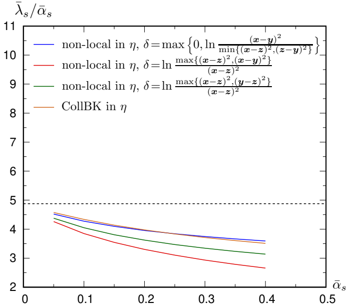

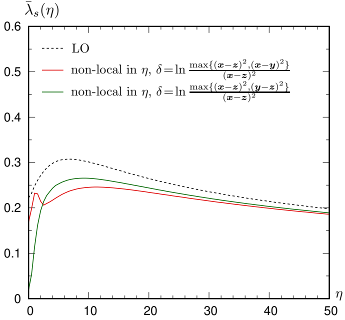

- Left: fixed coupling: a reduction of $20 \div 30\%$ w.r.t. LO
- Right: running coupling: $\lambda_s \simeq 0.20 \div 0.25$
- $\bar{\alpha}(r_{\min})$ where $r_{\min} = \min\{|\boldsymbol{x}-\boldsymbol{y}|, |\boldsymbol{x}-\boldsymbol{z}|, |\boldsymbol{y}-\boldsymbol{z}|\}$

BK evolution in η: saturation exponent

- $\lambda_s \equiv \frac{\mathrm{d}\ln Q_s^2}{\mathrm{d}\eta}$: the speed of the saturation front in η
  - recall: LO result $\lambda_s \simeq 4.88\bar{\alpha}$ (way too large)

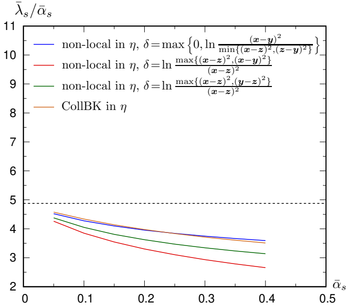

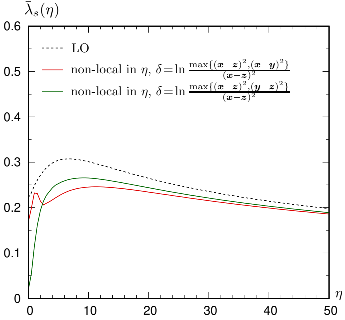

  - Left: fixed coupling: a reduction of $20 \div 30\%$ w.r.t. LO
  - Right: running coupling: $\lambda_s \simeq 0.20 \div 0.25$
  - $\bar{\alpha}(r_{\min})$ where $r_{\min} = \min\{|\boldsymbol{x}-\boldsymbol{y}|, |\boldsymbol{x}-\boldsymbol{z}|, |\boldsymbol{y}-\boldsymbol{z}|\}$
- The main reduction comes from the use of a running coupling